Zhijian Liu[1,2]
Di Li[2]
Maryam Saffarian[3]
Tzuen-Rong Tzeng[3]
Yongxin Song[1]
Xinxiang Pan[1]
Xiangchun Xuan[2]

[1]College of Marine Engineering, Dalian Maritime University, Dalian, P. R. China
[2]Department of Mechanical Engineering, Clemson University, Clemson, SC, USA
[3]Department of Biological Sciences, Clemson University, Clemson, SC, USA

Received May 7, 2018
Revised July 1, 2018
Accepted July 2, 2018

Research Article

Revisit of wall-induced lateral migration in particle electrophoresis through a straight rectangular microchannel: Effects of particle zeta potential

Previous studies have reported a lateral migration in particle electrophoresis through a straight rectangular microchannel. This phenomenon arises from the inherent wall-induced electrical lift that can be exploited to focus and separate particles for microfluidic applications. Such a dielectrophoretic-like force has been recently found to vary with the buffer concentration. We demonstrate in this work that the particle zeta potential also has a significant effect on the wall-induced electrical lift. We perform an experimental study of the lateral migration of equal-sized polystyrene particles with varying surface charges under identical electrokinetic flow conditions. Surprisingly, an enhanced focusing is observed for particles with a faster electrokinetic motion, which indicates a substantially larger electrical lift for particles with a smaller zeta potential. We speculate this phenomenon may be correlated with the particle surface conduction that is a strong function of particle and fluid properties.

Keywords:
Electrical lift / Particle focusing / Surface conduction / Electrokinetics / Microfluidics
DOI 10.1002/elps.201800198

1 Introduction

Electrokinetic flow has been widely used to transport liquids via electro-osmosis and particles (a general term of, for example, rigid particles, soft vesicles, cells, and viruses etc.) via electrophoresis in microchannels for microfluidic applications [1, 2]. Its velocity is parallel to (either along with or against) the applied electric field and proportional to the field magnitude via the electrokinetic mobility [3, 4]. Therefore, pure electrokinetic particle transport should be along the axis direction in straight microchannels regardless of the cross-sectional shape [5]. However, recent studies have both theoretically [6–10] and experimentally [11–15] demonstrated the occurrence of a dielectrophoretic-like force in electrokinetic flow that pushes particles away from any channel walls. This electrically originated lift force, similar to the function of the flow-induced inertial lift [16, 17] and elastic lift [18, 19], has been utilized to implement the three-dimensional electrokinetic focusing of particles in straight rectangular microchannels [20]. It has also been used to separate particles of different diameters due to its strong dependence on particle size [21–23]. Moreover, the electrical lift has been demonstrated to separate particles based on the difference in surface charge [23, 24], or equivalently, the particle zeta potential that has a direct impact on the electrokinetic motion [25].

We demonstrate in this work that the particle zeta potential also has a strong influence on the wall-induced electrical lift. This dependence was predicted in a recent theoretical paper from Yariv [26] who extended his earlier asymptotic analysis [6] to consider the effect of surface conduction on the electrical lift. His revised formula predicts a non-monotonic dependence of the electrical lift on a dimensionless Dukhin number [27], which is a complex function of both the particle zeta potential and the fluid ionic concentration. The effect of electrolyte concentration on the wall-induced electrical lift was experimentally studied by our group [28]. We observed in that work a significantly enhanced electrokinetic focusing of polystyrene particles in a straight rectangular microchannel when the molar concentration of the buffer solution was decreased. Interestingly, the electrokinetic particle mobility was found to increase logarithmically with the decrease of buffer concentration (consistent with the data in the literature [29]), which should diminish the electrokinetic particle focusing due to the reduced action time of the electrical lift. This work is aimed to experimentally study the effect of particle zeta potential on wall-induced lateral migration in particle electrophoresis through a straight rectangular microchannel. We test equal-sized spherical polystyrene particles with

Correspondence: Professor Xiangchun Xuan, Department of Mechanical Engineering, Clemson University, Clemson, SC 29634-0921, USA
Fax: +1-864-656-7299
E-mail: xcxuan@clemson.edu

Color Online: See the article online to view Figs. 1–5 in color.

various functionalized surfaces under identical electrokinetic flow conditions.

2 Materials and methods

2.1 Materials

The rectangular microchannel was fabricated with polydimethylsiloxane using the standard soft lithography technique. The detailed fabrication procedure can be referred to Li et al. [22]. The 2 cm long straight channel was measured 65 μm wide and 25 μm high. It has an expansion region at each end with an array of posts for filtration of debris. Four types of spherical polystyrene particles (with a density of 1.05 g/cm^3) were tested in our experiment, which were purchased from different companies including Bangs Laboratories Inc. (named as Bangs hereafter), Duke Scientific Corp. (Duke), Sigma-Aldrich Corp. (Sigma), and Thermo Scientific Inc. (Thermo). They have either plain or functioned (i.e., fluorescent) surfaces, and have a diameter of either 10 or (approximately) 5 μm. The uniformity of every type of particle is less than 5%. The detailed information of these particles is presented in Table 1. The four types of particles were each re-suspended in a phosphate buffer solution of either 1 mM or 0.1 mM concentration with pH ≈ 7. The particle concentration was kept low (less than 0.1% in weight ratio) to minimize particle-particle interactions. A small amount of Tween 20 (0.5% in volume, Fisher Scientific) was added into each suspension to reduce particle adhesions and aggregations.

2.2 Methods

The electrokinetic motion of particles was driven by a direct current (DC) electric field that was supplied by a high-voltage power supply (Glassman High Voltage Inc., High Bridge) through platinum electrodes inserted into the end-channel reservoirs. The electric field magnitude was limited to be no more than 500 V/cm in any test, at which the maximum temperature rise due to Joule heating, $\Delta T = \sigma E^2 D^2/k$ (where σ, E, D and k are the fluid electric conductivity, electric field magnitude, channel hydraulic diameter, and fluid thermal conductivity, respectively) [30], was estimated to be less than 0.1 K in 1 mM buffer solution (even smaller in 0.1 mM solution). The liquid heights in the two reservoirs were carefully balanced prior to every test to minimize the pressure-driven flow. Moreover, the duration of every test was limited to 1 min to avoid any significant back flows due to electro-osmosis-induced liquid level changes in the end-channel reservoirs [31], and as well as to avoid significant Joule heating effects [32].

Table 1. Spherical polystyrene particles used in the experiment

Name	Functionality	Diameter (μm)	Company
Sigma	plain	5.0/10.0	Sigma-Aldrich Corp.
Bangs	green fluorescent	4.2/9.8	Bangs Laboratories Inc.
Thermo	green fluorescent	4.8/9.9	Thermo Scientific Inc.
Duke	green fluorescent	5.0/9.9	Duke Scientific Corp.

Particle motion was visualized through an inverted microscope (Nikon Eclipse TE2000U, Nikon Instruments, Lewisville, TX) in conjunction with a CCD camera (Nikon DS-Qi1MC) under a bright-field illumination. Digital videos were recorded at a rate of around 15 frames/s with an exposure time of 1 ms. The acquired digital images had a resolution of 640 × 512 pixels with each pixel representing 1.47 μm (note: the smallest particle in our experiment had a diameter of 4.2 μm). The particle streak images were obtained by stacking a sequence of snapshot images using the Nikon imaging software (NIS-Elements AR 3.22). The electrokinetic velocity of particles was measured by tracking single particle positions with time on the acquired top-view images in the main-body of the microchannel (i.e., away from the channel ends). This measurement was done for 3–5 individual particles in each test and repeated for at least two tests performed in different days. The average of all the measured values (typically vary within the error of ±10%) was used as the electrokinetic velocity of the particles in a specific solution under a specific DC electric field. The electrokinetic mobility of particles was then determined from the slope of the linear trendline of the experimentally determined particle velocities vs. electric field in Microsoft Excel® [28]. The wall zeta potential of our polydimethylsiloxane-glass microchannel was measured using the current monitoring method [33]. The obtained average values (with an experimental error of around 10%) are about −85 mV in 1 mM buffer and −120 mV in 0.1 mM buffer, respectively. These numbers are found to be comparable to those calculated from the formula that was provided in the review article of Kirby and Hasselbrink [29]. With the known wall zeta potential, the particle zeta potential was then calculated from the measured electrokinetic particle mobility (see Eq. (5) in the section below).

3 Theory

Particles in an electro-osmotic fluid flow through a straight rectangular microchannel experience a wall-induced electrical lift, $\mathbf{F}_w$ [6],

$$\mathbf{F}_w = f_w\, \varepsilon a^2 E^2 \mathbf{n} \tag{1}$$

where f_w is a dimensionless coefficient that depends on the particle-fluid-channel system, ε is the fluid permittivity, a is the particle radius, and $\mathbf{n}$ is the unit vector normal to the wall pointing into the fluid. In this work, f_w is a function of the system geometry that includes the particle blockage ratio, $\beta = a/w$, and the particle eccentricity, $\epsilon = \delta/w$, where w is the microchannel half-width and δ is the particle's off-center distance [6–15]. It also depends on the surface conduction effect [26] that is often characterized by the Dukhin number, Du, which relates the particle surface conductivity to the

fluid bulk conductivity and is a function of particle (e.g., size and zeta potential) and fluid (e.g., ionic concentration and mobility) properties [27],

$$Du = \frac{2}{\kappa a}(1+2\alpha)\left[\cosh\left(\frac{ze\zeta_p}{2k_BT}\right)-1\right]\left(1+\frac{K^{\sigma i}}{K^{\sigma d}}\right) \quad (2)$$

where κ is the so-called Debye-Huckel parameter [25], $\alpha = (\varepsilon/\eta D)(k_BT/ze)^2$ is a dimensionless number [26] (note η is the fluid viscosity, D is the (assumed) equal cationic and anionic diffusivity, k_BT is the Boltzmann temperature, z is the ionic valence, and e is the proton charge), ζ_p is the particle zeta potential, $K^{\sigma i}$ is the surface conductivity due to the stagnant layer charge, and $K^{\sigma d}$ is the surface conductivity due to the diffuse layer charge. Therefore, the surface conduction effect is a strong positive function of the particle zeta potential. The lateral particle migration, $\mathbf{U}_w$, is obtained by balancing the electrical lift in Eq. (1) with Stokes' drag [34],

$$\mathbf{U}_w = \frac{f_w}{f_D}\frac{\varepsilon a^2 E^2}{6\pi\eta a}\mathbf{n} \quad (3)$$

where f_D is the drag coefficient that accounts for the wall effects on particle motion, and η is the fluid viscosity. Note that the inertial focusing effect on particle migration is negligible in our experiments as the Reynolds number is much smaller than 1 [16, 17].

The wall-induced transverse dielectrophoretic-like particle migration, $\mathbf{U}_w$, competes with the streamwise electrokinetic particle motion, $\mathbf{U}_{ek}$,

$$\mathbf{U}_{ek} = f_E\,\mu_{ek}\mathbf{E} \quad (4)$$

$$\mu_{ek} = \frac{\varepsilon(\zeta_p-\zeta_w)}{\eta} \quad (5)$$

where f_E is a dimensionless coefficient [5] that, similar to the coefficient f_w in Eq. (1), depends also on the system geometry [5, 15, 35–42] and surface conduction [26], μ_{ek} is the traditionally defined as electrokinetic particle mobility under the limit of thin electric double layers (which is in the order of 10 nm in our experiments) [1–3], $\mathbf{E}$ is the electric field vector, and ζ_p and ζ_w are the zeta potentials of the particle and channel wall, respectively. We note that $f_E \approx 1$ [5, 25] unless the particle closely fits a microchannel or nearly touches a channel wall [35–42] or the particle Dukhin number is on the order of 1 [26]. The lateral migration distance is dependent on the ratio of the cross-stream and streamwise particle speeds,

$$\frac{U_w}{U_{ek}} = \frac{aE}{6\pi f_D}\frac{f_w}{(\zeta_p-\zeta_w)f_E} \quad (6)$$

Therefore, the electrokinetic particle focusing is a positive function of particle size, a, and electric field, E, as demonstrated in our previous studies [11, 20]. Its dependence on the particle zeta potential, ζ_p, is, however, not straightforward from Eq. (6) as the latter also affects the dimensionless coefficients f_w and f_E as noted above [26].

4 Results and discussion

4.1 Particles in 1 mM buffer

We first studied the electrokinetic transport of four types of 10 μm-diameter polystyrene particles from Sigma, Bangs, Thermo, and Duke, respectively, in the flow of 1 mM phosphate buffer through the same straight rectangular microchannel, i.e., under identical flow conditions. Figure 1 compares the top-view images of these particles under varying DC electric fields. Every type of particles are randomly dispersed at the channel inlet while their distributions at the channel outlet are significantly different. Specifically, the Sigma particles apparently migrate toward the channel centerline exhibiting the strongest electrokinetic focusing among all the particles. Next to them are the Bangs particles and then the Thermo particles, whose focusing both get weaker but still visible on the images. As predicted in Eq. (6), such a wall-induced electrokinetic particle focusing increases at higher electric fields for each of these three types of particles in Figure 1. In contrast, however, the Duke particles appear to experience little focusing effect even at the highest electric field in our tests.

The observed trends of electrokinetic focusing for the four type of particles in Fig. 1 are quantitatively illustrated by the line plots of the measured particle stream width vs. electric field magnitude in Fig. 2A. All data points were

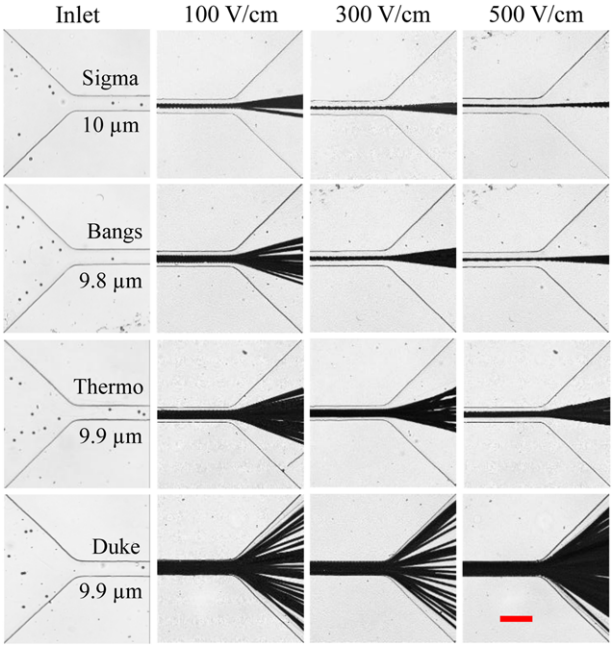

Figure 1. Top-view images of 10 μm-diameter Sigma, Bangs, Thermo and Duke particles in the electrokinetic flow of 1 mM phosphate buffer at the inlet (left column, snapshot) and outlet (all other columns, superimposed) of the straight rectangular microchannel. The values of the average DC electric field across the channel length are labeled on top of the images. Particles travel from left to right in all images. The scale bar represents 100 μm.

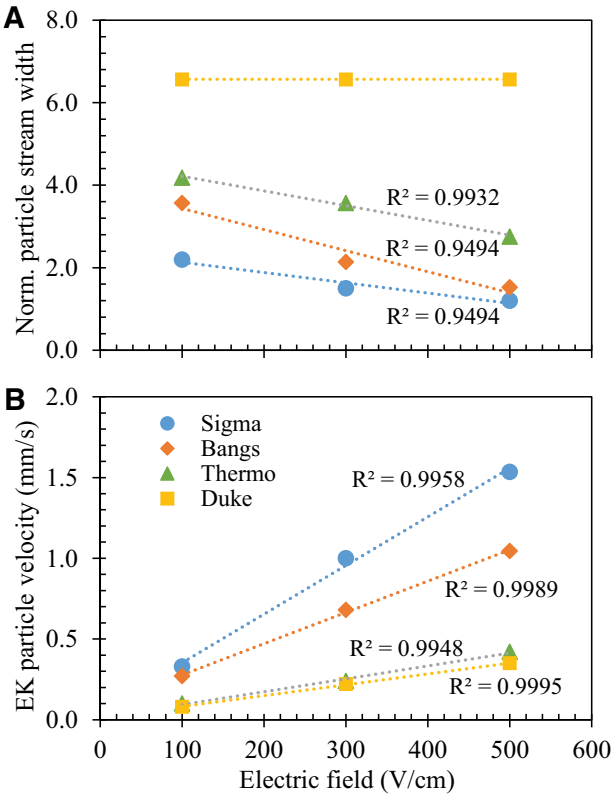

Figure 2. Electrokinetic motion of 10 μm-diameter Sigma, Bangs, Thermo and Duke particles in 1 mM phosphate buffer under different DC electric fields: (A) particle stream width at the channel outlet (normalized by the corresponding particle diameter); (B) electrokinetic particle velocity. In each plot, the symbols represent the experimental data that were obtained directly from the images (or videos) in Figure 1. The dashed lines are the linear regression lines of the experimental data points with the corresponding R^2 values being highlighted except that for the exactly zero-slope line of Duke particle stream width in (A).

obtained from the images in Fig. 1 and normalized by the corresponding particle diameter. Interestingly, each plot in Fig. 2A follows an approximately linear relationship with a negative (or zero for the Duke particles) slope, which is demonstrated by the linear regression line (dashed line with the R^2 value being highlighted) of the experimental data points (symbols). This is consistent with our previous experimental observations [11, 20], and also consistent with the prediction of Eq. (6) considering the positive linear dependence of the lateral particle migration distance on the electric field. However, the values and slopes of the four line plots in Fig. 2A are different from each other because of the dissimilar zeta potential values of the four types of particles [see Eq. (6)]. To quantify this effect, we measured the electrokinetic velocities of each type of particles at the electric fields of 100, 300, and 500 V/cm, respectively, which are presented in Fig. 2B. As expected from Eq. (4), the electrokinetic particle velocity is linearly proportional to the electric field magnitude (see the linear regression lines in Fig. 2B where the R^2 values are included). However, surprisingly, the faster the particle moves (Fig. 2B,) the better electrokinetic focusing is achieved (Fig. 2A). For instance, the slowest Duke particles exhibits no electrokinetic focusing while the fastest Sigma particles experiences the best focusing effect.

To better illustrate this point, we determined the electrokinetic mobility of each type of particles from Eq. (4) using the experimentally measured particle velocity with the assumption of $f_E = 1$ as noted above. We then estimated the particle zeta potential using the method described in section 3.2. As viewed from Fig. 3, the Sigma particles have the largest electrokinetic mobility that is followed by the Bangs, Thermo, and Duke particles in the decreasing order. This trend is opposite to that of the measured stream width for the four types of particles in Figure 3 (under 300 V/cm). Therefore, the wall-induced lateral migration of the Sigma particles should be substantially greater than that of any other equal-sized particles, which in our tests can only be attributed to the difference in the particle zeta potential. As they all move along the direction of the DC electric field with a positive electrokinetic mobility, the four types of particles should each have a lower zeta potential magnitude than the channel wall (both are negative). Moreover, a larger electrokinetic mobility corresponds to a smaller magnitude of (negative) particle zeta potential. Therefore, the Sigma, Bangs, Thermo, and Duke particles in order should have an increasing zeta potential magnitude as illustrated in Fig. 3 (see the horizontal axis), which in turn yields a stronger surface conduction effect [27], as indicated by the greater Dukhin number, *Du*, in Eq. (2). We estimated the magnitude of particle *Du* by assuming the stagnant layer to diffuse layer conductivity ratio (associated with both the surface charge and the microscopic surface structure of particles [25–27, 43, 44]), $K^{\sigma i}/K^{\sigma d} = 10$. We found that the particle *Du* increases approximately from 0.05 to 0.2, which may be the reason behind the significant increase in

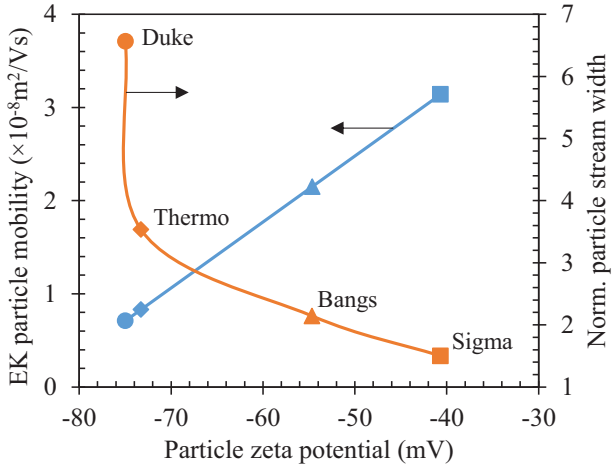

Figure 3. Experimentally measured electrokinetic mobility and stream width at the channel outlet (under 300 V/cm, normalized by the particle diameter) for 10 μm-diameter Sigma, Bangs, Thermo and Duke particles in 1 mM phosphate buffer. The particle zeta potentials were estimated from the electrokinetic mobility values using Eq. (5).

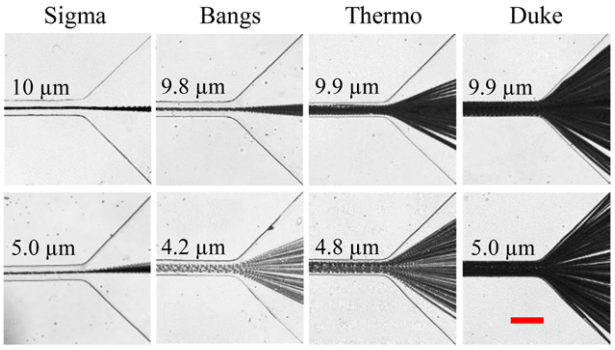

Figure 4. Top-view images of 10 μm- (upper row) and 5 μm- (lower row) diameter Sigma, Bangs, Thermo and Duke particles in the electrokinetic flow of 0.1 mM phosphate buffer at the outlet of a straight rectangular microchannel. The average DC electric field across the channel length was fixed at 300 V/cm. Particles travel from left to right in all images. The scale bar represents 100 μm.

the particle stream width (or equivalently the reduced particle focusing), shown in Fig. 3, if the dimensionless coefficient, f_w, in Eq. (1) and Eq. (6) decreases at an increasing Du [26].

4.2 Particles in 0.1 mM buffer

To further verify the above demonstrated phenomena, we also studied the electrokinetic transport of 10 μm-diameter Sigma, Bangs, Thermo, and Duke particles in the flow of 0.1 mM phosphate buffer through the same straight rectangular microchannel. Moreover, we repeated the tests for approximately 5 μm particles from the same companies under identical experimental conditions. Figure 4 shows the top-view images at the channel outlet from these tests under the DC electric field of 300 V/cm. Consistent with the observation of 10 μm particles in 1 mM buffer (Fig. 1, see the images in the third column), the Sigma particles (both 5 μm and 10 μm) still achieve the best electrokinetic focusing in 0.1 mM buffer solution. Next to them are the Bangs, Thermo, and Duke particles in the order of decreasing focusing effect, which is also consistent with Fig. 1.

Figure 5 presents the experimentally measured electrokinetic mobility and the corresponding zeta potential (see the horizontal axis) for each type of particles in 0.1 mM buffer. We find that 5 μm and 10 μm particles from the same company have approximately similar electrokinetic mobilities and in turn zeta potentials, whose values are all greater than those in 1 mM buffer. Similar to the trend observed in 1 mM buffer (Figure 3), the Sigma particles still move the fastest in 0.1 mM buffer, leading to an increasing zeta potential magnitude for the Sigma, Bangs, Thermo and Duke particles in order. This is again contradictory to the trend of the measured stream width for the four types of particles in Figure 5, which, as explained in the preceding section, may be correlated with the stronger surface conduction effect under a greater zeta potential value [27]. In addition, the electrokinetic focusing of 10 μm particles is apparently better than that of 5 μm

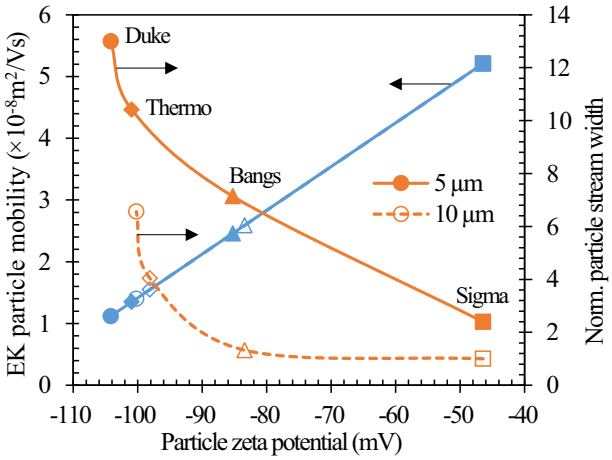

Figure 5. Experimentally measured electrokinetic mobility and stream width at the channel outlet (under 300 V/cm, normalized by the particle diameter) for 5 μm- (filled symbols with solid lines) and 10 μm- (hollow symbols with dashed lines) diameter Sigma, Bangs, Thermo, and Duke particles in 0.1 mM phosphate buffer.

particles if they are from the same company. This is a direct result of the positive dependence of the wall-induced lateral migration on particle size in Eq. (6), consistent with previous studies [11, 20–23].

5 Concluding remarks

We have experimentally studied the electrokinetic transport of four types of equal-sized polystyrene particles in the flow of buffer solutions through a straight rectangular microchannel. The lateral particle migration due to the wall-induced electrical lift is found to be a strong function of the particle zeta potential. Specifically, the particles that have a larger electrokinetic mobility experience an enhanced focusing effect under the identical flow conditions. This indicates that the increase in the lateral particle migration should be quicker than that in the axial electrokinetic motion when the magnitude of the negative particle zeta potential is decreased. A similar trend was also reported in our recent study of the buffer concentration effect [28], where the wall-induced electrokinetic focusing was found stronger for particles that move faster in lower-concentration buffers. The exact mechanism behind each of these phenomena is currently unclear, which is speculated to relate to the surface conduction effect that depends on the particle and fluid properties [26]. We hope our experiments in both, this work and the recent one [28] will stimulate more theoretical (or numerical) studies for potential physical explanations of the observed phenomena.

This work was supported in part by China Scholarship Council (CSC)-State Scholarship Fund (Z.L.), Fundamental Research Funds for the Central Universities under Grants No. 3132018254 (Z.L.) and 3132016325 (Y.S.), National Natural Science Foundation of China under Grants No. 51679023

(Y.S.) and 51479020 (X.P.), and NSF under Grant No. CBET-1704379 (X.X.).

The authors have declared no conflict of interest.

6 References

[1] Chang, H. C., Yeo, L. Y., *Electrokinetically-Driven Microfluidics and Nanofluidics*, Cambridge University Press, New York, USA 2009.

[2] Kang, Y., Li, D., *Microfluid. Nanofluid.* 2009, *6*, 431–460.

[3] Li, D., *Electrokinetics in Microfluidics*, Academic Press, Burlington, MA, USA 2004.

[4] Xuan, X., Raghibizadeh, S., Li, D., *J. Colloid Interf. Sci.* 2006, *296*, 743–748.

[5] Anderson, J. L. *Annu. Rev. Fluid. Mech.* 1989, *21*, 61–99.

[6] Yariv, E., *Phys. Fluid.* 2006, *18*, 031702.

[7] Zhao, H., Bau, H., *Langmuir* 2007, *23*, 4053–4063.

[8] Young, E., Li, D., *Langmuir* 2005, *21*, 12037–12046.

[9] Lo, Y. J., Lei, U., *Appl. Phys. Lett.* 2009, *95*, 253701.

[10] Kang, S., *J. Electrostat.* 2015, *76*, 159–170.

[11] Liang, L., Ai, Y., Zhu, J., Qian, S., Xuan, X., *J. Colloid Interf. Sci.* 2010, *347*, 142–146.

[12] Lo, Y. J., Lei, U., *Appl. Phys. Lett.* 2010, *97*, 093702.

[13] Yoda, M., Kazoe, Y., *Phys. Fluid.* 2011, *23*, 111301.

[14] Kazoe, Y., Yoda, M., *Langmuir* 2011, *27*, 11481–11488.

[15] Liang, Q., Zhao, C., Yang, C., *Electrophoresis* 2015, *36*, 731–736.

[16] Amini, H., Lee, W., Di Carlo, D., *Lab Chip* 2014, *14*, 2739–2761.

[17] Zhang, J., Yan, S., Yuan, D., Alici, G., Nguyen, N. T., Warkiani, M. E., Li, W., *Lab Chip* 2016, *16*, 10–34.

[18] Lu, X., Liu, C., Hu, G., Xuan, X., *J. Colloid Interf. Sci.* 2017, *500*, 182–201.

[19] Liu, C., Hu, G., *Micromachines* 2017, *8*, 73.

[20] Liang, L., Qian, S., Xuan, X., *J. Colloid Interf. Sci.* 2010, *350*, 377–379.

[21] Lu, X., Hsu, J. P., Xuan, X., *Langmuir* 2015, *31*, 620–627.

[22] Li, D., Lu, X., Song, Y., Wang, J., Li, D., Xuan, X., *Biomicrofluid.* 2016, *10*, 054104.

[23] Li, M., Li, D., *J. Chromatography A* 2017, *1501*, 151–160.

[24] Thomas, C., Lu, X., Todd, A., Raval, Y., Tzeng, T., Song, Y., Wang, J., Li, D., Xuan, X., *Electrophoresis* 2017, *38*, 320–326.

[25] Hunter, R. J., *Zeta Potential in Colloid Science*, Academic Press, New York 1981.

[26] Yariv, E., *Soft Matt.* 2016, *12*, 6277–6284.

[27] Delgado, A. V., González-Caballero, F., Hunter, R. J., Koopal, L. K., Lyklema, J., *J. Colloid Interf. Sci.* 2007, *309*, 194–224.

[28] Liu, Z., Li, D., Song, Y., Pan, X., Li, D., Xuan, X., *Phys. Fluid.* 2017, *29*, 102001.

[29] Kirby, B. J., *Electrophoresis* 2004, *25*, 203–213.

[30] Ramos, A., Morgan, H., Green, N. G., Castellanos, A., *J. Phys. D* 1998, *31*, 2338–2353.

[31] Yan, D., Yang, C., Huang, X., *Microfluid. Nanofluid.* 2007, *3*, 333–340.

[32] Xuan, X., *Electrophoresis* 2008, *29*, 33–43.

[33] Sze, A., Erickson, D., Ren, L., Li, D. *J. Colloid Interf. Sci.* 2003, *261*, 402–410.

[34] Happel, J., Brenner, H., *Low Reynolds Number Hydrodynamics*, Springer Press, The Hague, The Netherlands 1973.

[35] Keh, H. J., Anderson, J. A., *J. Fluid. Mech.* 1985, *153*, 417–439.

[36] Yariv, E., Brenner, H., *Phys. Fluid.* 2002, *14*, 3354–3357.

[37] Yariv, E., Brenner, H., *SIAM J. Appl. Math.* 2003, *64*, 423–441.

[38] Ye, C., Xuan, X., Li, D., *Microfluid. Nanofluid.* 2005, *1*, 234–241.

[39] Hsu, J. P., Kuo, C. C., *J. Phys. Chem. B* 2006, *110*, 17607–17615.

[40] Unni, H. N., Keh, H. J., Yang, C., *Electrophoresis* 2007, *28*, 658–664.

[41] Ai, Y., Beskok, A., Gauthier, D. T., Joo, S. W., Qian, S., *Biomicrofluid.* 2010, *3*, 044110.

[42] Xuan, X., Ye, C., Li, D., *J. Colloid Interf. Sci.* 2005, *289*, 286–290.

[43] Schnitzer, O., Yariv, E., *Phys. Rev. E* 2012, *86*, 021503.

[44] Saville, D. A., *Annu. Rev. Fluid Mech.* 1977, *9*, 321–337.

